Journal of Sound and Vibration (2002) **258**(5), 987–999
doi:10.1006/jsvi.2002.5184, available online at http://www.idealibrary.com on IDEAL®

BEAM VIBRATIONS WITH AN ARBITRARY NUMBER OF CRACKS

H. P. Lin, S. C. Chang and J. D. Wu

Department of Vehicle Engineering, Da-Yeh University, 112. *Shan-Jiau Road, Da-Tsuen, Chang-Hua* 51505*, Taiwan, Republic of China. E-mail: linhp@mail.dyu.edu.tw*

(*Received* 11 *January* 2002)

1. INTRODUCTION

The dynamics of cracked structures has been a topic of active research during the last decade. When a structural component is subjected to a crack, the crack induces a local flexibility which is a function of the crack depth, thereby changing its dynamic behavior and its stability characteristics [1]. Some researches have proposed techniques to estimate the effects on the eigenparameters on these structures (direct methods), while others have dealt with the problem of detecting, locating and quantifying the extent of damage (inverse problem).

The dynamic behavior of the cracked structures was studied by several analytical and numerical methods [2–9]. Dimarogonas presents a state of review on the dynamics of the cracked structures [10]. Many works in this fields deal with the cracked beam, subject to various boundary conditions. A complete cracked beam vibration theory is also developed by Chondros and Dimarogonas [11] for the lateral vibration of cracked Euler–Bernoulli beam with single-edge or double-edge open cracks. In reference [11], the crack region as a local flexibility was expressed by a crack disturbance function $f(x, z)$ which could be derived from the stress intensity factors in the theory of fracture mechanics. In most of the previous studies, the model of Euler–Bernoulli beam theory by deriving the differential equation and the associated boundary conditions for a uniform Euler–Bernoulli beam containing one or two cracks are often used and discussed.

Some of the researches evaluate the change in eigensolutions due to the presence of cracks on beam by finite element methods. In some other articles, the beam was subdivided into several beams, separated from one another by a crack, which was represented through a massless rotational spring [2–4, 6, 9]. In both of the previous methods, finally, it is possible to evaluate natural frequencies simply by finding roots of the *high order determinant* of the coefficient matrix of the linear system. In finite element methods, the order of the determinant is increased as the degree of freedom (nodes) is increased. Usually, this method leads to high order determinant if the accuracy of the eigensolutions is required. On the other hand, the general solution for the eigenfunctions of every beam contains four unknown constants and this leads to a system of $(4n + 4)$ equations in case of n cracks [7, 8]. Usually, it is not easy to construct the linear system using the method proposed in references [7, 8] for a general case of n cracks. This is the main reason for most of the cases that only one or two cracks were considered in detail, without attempting to provide a solution for a more general situation except in reference [2].

This investigation presents a hybrid analytical/numerical method that permits the efficient computation of the eigensolutions for an arbitrary number of cracks of a beam

0022-460X/02/$35.00

with various boundary conditions. The method is based on the use of massless rotational spring to present the cracks, and by the patching conditions of each crack, the relationships of the four integration constants of the eigenfunctions between adjacent sub-beams can be determined [12]. By using the transfer matrix, as a consequence, the whole system has only four unknown constants which can be solved through the satisfaction of four boundary conditions. An analytical form of eigenvalue problem is introduced which is solved using closed form, transfer matrix methods in this article.

2. THEORETICAL MODEL

An Euler Bernoulli beam of length L and with k open cracks is considered as in Figure 1. It is assumed that the cracks are located at points $X_1, X_2, ..., X_k$ such that $0 < X_1 < X_2 < \cdots < X_k < L$. The vibration amplitudes of the transverse displacements of the beam are denoted by $Y_j(X, T)$ on the interval $X_{j-1} < X < X_j$, where the sub-index j represents the jth segment and $j = 1, 2, \ldots, k+1$ (refer to Figure 1). The entire beam (whole domain) is now divided into $(k+1)$ segments (sub-domains) with lengths $l_1, l_2, \ldots, l_{k+1}$, respectively, which are separated by k cracks. According to the literature in references [2, 3, 11], the equation of motion for each segment, assume with uniform cross-section, is

$$EI \frac{\partial^4 Y_i(X,T)}{\partial X^4} + \rho A \frac{\partial^2 Y_i(X,T)}{\partial T^2} = 0, \quad X_{i-1} < X < X_i, \;\; i = 1, 2, \ldots, k+1, \tag{1}$$

where E is Young's modulus of the material, I is the moment of inertia of the beam cross-section, ρ is the density of material and A is the cross-section area of the beam.

The boundary conditions of the beam for the simply supported case are:

$$Y(0,T) = Y(L,T) = 0, \quad Y''(0,T) = Y''(L,T) = 0. \tag{2a, b}$$

The "patching conditions" enforce continuities of the displacement field, bending moment and shear force, respectively, across each crack and can be expressed as

$$Y_i(X_i^-, T) = Y_{i+1}(X_i^+, T), \quad Y_i''(X_i^-, T) = Y_{i+1}''(X_i^+, T), \tag{2c, d}$$

$$Y_i'''(X_i^-, T) = Y_{i+1}'''(X_i^+, T), \quad i = 1, 2, \ldots, k. \tag{2e}$$

Moreover, a discontinuity into the slope of the beam across each crack exists and can be expressed [3] as

$$Y_{i+1}'(X_i^+, T) - Y_i'(X_i^-, T) = \theta_i L Y_{i+1}''(X_i^+, T), \quad i = 1, 2, \ldots, k, \tag{2f}$$

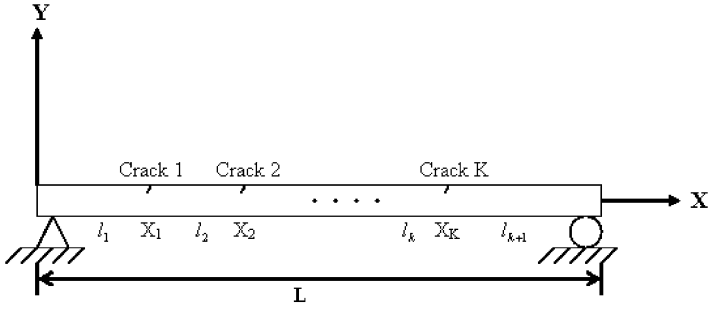

Figure 1. A beam with k cracks located at positions $X_1, X_2, \ldots, X_K$, respectively, and the sub-domains are $l_1, l_2, \ldots, l_k, l_{k+1}$ where $l_1 + l_2 + \cdots + l_k + l_{k+1} = L$.

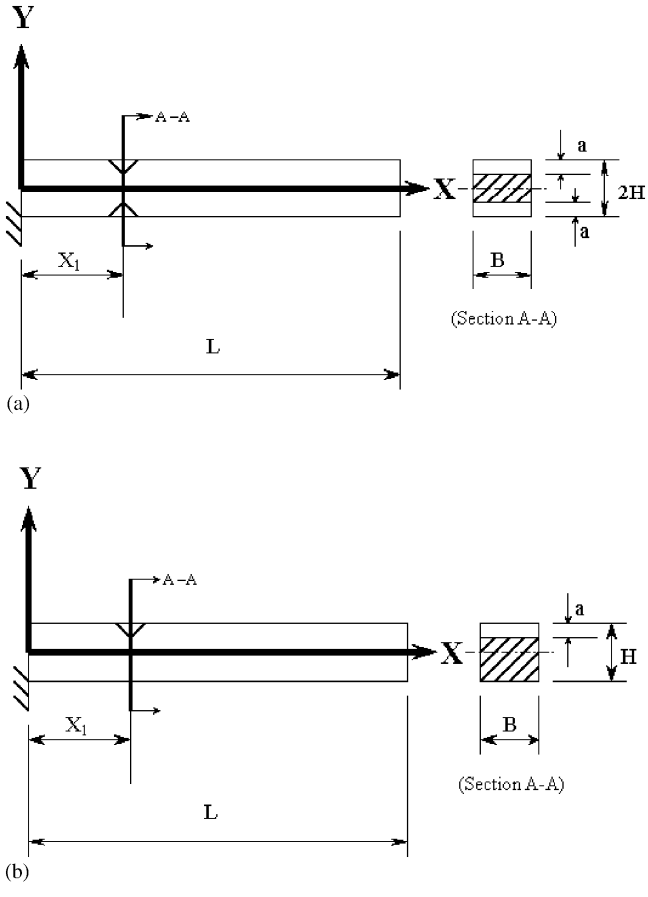

Figure 2. (a) Sketch figure of a double-side crack and (b) sketch figure of a single-side crack.

where θ_i is the non-dimensional ith crack section flexibility which are functions of the crack extent [4, 7]. For double-side open cracks [7], refer to Figure 2(a) as

$$\theta_i = 6\pi\bar{\gamma}_i^2 f_D(\bar{\gamma}_i)\left(\frac{H}{L}\right), \tag{3a}$$

where $\bar{\gamma}_i = a_i/H$, a_i is the depth of the ith crack and

$$f_D(\bar{\gamma}_i) = 0{\cdot}5335 - 0{\cdot}929\bar{\gamma}_i + 3{\cdot}500\bar{\gamma}_i^2 - 3{\cdot}181\bar{\gamma}_i^3 + 5{\cdot}793\bar{\gamma}_i{}^4. \tag{3b}$$

For single-side open cracks, refer to Figure 2(b) [7]

$$\theta_i = 6\pi\bar{\gamma}_i^2 f_J(\bar{\gamma}_i)\left(\frac{H}{L}\right), \tag{3c}$$

$$f_J(\bar{\gamma}_i) = 0{\cdot}6384 - 1{\cdot}035\bar{\gamma}_i + 3{\cdot}7201\bar{\gamma}_i^2 - 5{\cdot}1773\bar{\gamma}_i^3 + 7{\cdot}553\bar{\gamma}_i^4 - 7{\cdot}332\bar{\gamma}_i^5 + 2{\cdot}4909\bar{\gamma}_i{}^6. \tag{3d}$$

For the cases of closing cracks, the model is the same except the expressions for different functions of $f_{D,J}(\bar{\gamma}_i)$ [1].

In the above, the following quantities are introduced:

$$y = \frac{Y}{L}, \quad x = \frac{X}{L}, \quad t = \frac{T}{\sqrt{L}}. \tag{4}$$

Thus, in each segment, equation (1) can then be expressed in the non-dimensional form as

$$\frac{EI}{L^3}\frac{\partial^4 y_i(x,t)}{\partial x^4} + \rho A \frac{\partial^2 y_i(x,t)}{\partial t^2} = 0, \quad x_{i-1} < x < x_i, \;\; i = 1, 2, ..., k+1. \tag{5}$$

The non-dimensional "patching conditions" from equations (2c) to (2f) are:

$$y_i(x_i^-, t) = y_{i+1}(x_i^+, t), \quad y_i''(x_i^-, t) = y_{i+1}''(x_i^+, t), \tag{6a, b}$$

$$y_i'''(x_i^-, t) = y_{i+1}'''(x_i^+, t), \quad y_{i+1}'(x_i^+, t) - y_i'(x_i^-, t) = \theta_i y_{i+1}''(x_i^+, t), \tag{6c, d}$$

where $i = 1, 2, \ldots, k$ and θ_i is in equations (3a) and (3c) for double and single-sided open cracks respectively.

3. CALCULATION OF EIGENSOLUTIONS

The eigensolutions for the cases of commonly used different boundary conditions are derived. The solutions of the other boundary conditions can also be obtained easily through the similar procedure. Using the separable solutions: $y(x,t) = w(x)e^{j\omega t}$ in equation (5) leads to the associated eigenvalue problem

$$w_i''''(x) - \lambda^4 w_i(x) = 0, \quad x_{i-1} < x < x_i, \;\; i = 1, 2, \ldots, k+1, \tag{7}$$

where

$$\lambda^4 = \frac{\rho A \omega^2 L^3}{EI}. \tag{7a}$$

From equations (6a)–(6d), the corresponding patching conditions across each crack lead to

$$w_i(x_i^-) = w_{i+1}(x_i^+), \quad w_i''(x_i^-) = w_{i+1}''(x_i^+), \tag{8a, b}$$

$$w_i'''(x_i^-) = w_{i+1}'''(x_i^+), \quad w_{i+1}'(x_i^+) - w_i'(x_i^-) = \theta_i w_{i+1}''(x_i^+) \tag{8c, d}$$

for $i = 1, 2, \ldots, k$. A closed form solution to this eigenvalue problem can be obtained by employing transfer matrix methods [12–14]. The general solution of equation (7), for each segment, is

$$\begin{aligned} w_i(x) = {} & A_i \sin\lambda(x - x_{i-1}) + B_i \cos\lambda(x - x_{i-1}) + C_i \sinh\lambda(x - x_{i-1}) \\ & + D_i \cosh\lambda(x - x_{i-1}), \quad x_{i-1} < x < x_i, \;\; i = 1, 2, \ldots, k+1, \end{aligned} \tag{9}$$

where A_i, B_i, C_i and D_i are constants associated with the ith segment ($i = 1, 2, \ldots, k+1$). These constants in the (i+1)th segment (A_{i+1}, B_{i+1}, C_{i+1} and D_{i+1}) are related to those in the ith segment (A_i, B_i, C_i and D_i) through the patching conditions in equation (8a)–(8d) and can be expressed as

$$\begin{Bmatrix} A_{i+1} \\ B_{i+1} \\ C_{i+1} \\ D_{i+1} \end{Bmatrix} = \begin{bmatrix} t_{11} t_{12} t_{13} t_{14} \\ \vdots \\ \cdots t_{44} \end{bmatrix}^{(i)} \begin{Bmatrix} A_i \\ B_i \\ C_i \\ D_i \end{Bmatrix} = \underset{4\times4}{T^{(i)}} \begin{Bmatrix} A_i \\ B_i \\ C_i \\ D_i \end{Bmatrix}, \quad i = 1, 2, \ldots, k, \tag{10}$$

where $\underline{T}^{(i)}_{4\times4}$ is the 4×4 transfer matrix which depends on the eigenvalue λ and the elements is derived in Appendix A and are rewritten here as follows:

$$t_{11} = \cos \lambda l_i - \tfrac{1}{2}\theta_i\lambda \sin \lambda l_i, \quad t_{12} = -\sin \lambda l_i - \tfrac{1}{2}\theta_i\lambda \cos \lambda l_i, \tag{10a, b}$$

$$t_{13} = \tfrac{1}{2}\theta_i\lambda \sinh \lambda l_i, \qquad t_{14} = \tfrac{1}{2}\theta_i\lambda \cosh \lambda l_i, \tag{10c, d}$$

$$t_{21} = \sin \lambda l_i, \quad t_{22} = \cos \lambda l_i, \quad t_{23} = 0, \tag{10e–g}$$

$$t_{24} = 0, \quad t_{31} = -\tfrac{1}{2}\theta_i\lambda \sin \lambda l_i, \quad t_{32} = -\tfrac{1}{2}\theta_i\lambda \cos \lambda l_i \tag{10h–j}$$

$$t_{33} = \cosh \lambda l_i + \tfrac{1}{2}\theta_i\lambda \sinh \lambda l_i, \quad t_{34} = \sinh \lambda l_i + \tfrac{1}{2}\theta_i\lambda \cosh \lambda l_i, \tag{10k, l}$$

$$t_{41} = 0, \quad t_{42} = 0, \quad t_{43} = \sinh \lambda l_i, \tag{10m–o}$$

$$t_{44} = \cosh \lambda l_i. \tag{10p}$$

Through repeated application of equation (10), the four constants in the first segment (A_1, B_1, C_1 and D_1) can be mapped into those of the last segment, reducing the number of independent constants to four.

$$\begin{Bmatrix} A_{k+1} \\ B_{k+1} \\ C_{k+1} \\ D_{k+1} \end{Bmatrix} = \underline{T}^{(k)}_{4\times4} \begin{Bmatrix} A_k \\ B_k \\ C_k \\ D_k \end{Bmatrix} = \underline{T}^{(k)}_{4\times4}\underline{T}^{(k-1)}_{4\times4} \begin{Bmatrix} A_{k-1} \\ B_{k-1} \\ C_{k-1} \\ D_{k-1} \end{Bmatrix} = \underline{T}^{(k)}_{4\times4}\underline{T}^{(k-1)}_{4\times4} \cdots \underline{T}^{(1)}_{4\times4} \begin{Bmatrix} A_1 \\ B_1 \\ C_1 \\ D_1 \end{Bmatrix}. \tag{11}$$

These four remaining constants (A_1, B_1, C_1 and D_1) can be found through the satisfaction of the boundary conditions.

For the case of a simply supported beam, the corresponding boundary conditions of equations (2a) and (2b) can thus be expressed as follows:

$$Y(0, T) = 0 \rightarrow w(0) = 0, \tag{12a}$$

$$Y(L, T) = 0 \rightarrow w(1) = 0, \tag{12b}$$

$$Y''(0, T) = 0 \rightarrow w''(0) = 0, \tag{12c}$$

$$Y''(L, T) = 0 \rightarrow w''(1) = 0. \tag{12d}$$

Beginning with those at the left support, equations (9), (12a) and (12c), leads to

$$B_1 = 0 \quad \text{and} \quad D_1 = 0. \tag{13}$$

Satisfaction of the boundary conditions of equation (9) at the right supports, equations (12b) and (12d) requires

$$A_{k+1} \sin \lambda l_{k+1} + B_{k+1} \cos \lambda l_{k+1} + C_{k+1} \sinh \lambda l_{k+1} + D_{k+1} \cosh \lambda l_{k+1} = 0, \tag{14a}$$

$$-A_{k+1} \sin \lambda l_{k+1} - B_{k+1} \cos \lambda l_{k+1} + C_{k+1} \sinh \lambda l_{k+1} + D_{k+1} \cosh \lambda l_{k+1} = 0, \tag{14b}$$

which can be expressed in matrix form as

$$\begin{Bmatrix} 0 \\ 0 \end{Bmatrix} = \begin{bmatrix} \sin \lambda l_{k+1} & \cos \lambda l_{k+1} & \sinh \lambda l_{k+1} & \cosh \lambda l_{k+1} \\ -\sin \lambda l_{k+1} & -\cos \lambda l_{k+1} & \sinh \lambda l_{k+1} & \cosh \lambda l_{k+1} \end{bmatrix} \begin{Bmatrix} A_{k+1} \\ B_{k+1} \\ C_{k+1} \\ D_{k+1} \end{Bmatrix} = \underline{B}_{2\times4} \begin{Bmatrix} A_{k+1} \\ B_{k+1} \\ C_{k+1} \\ D_{k+1} \end{Bmatrix}, \tag{15}$$

where

$$\underline{B}_{2\times4} = \begin{bmatrix} \sin\lambda l_{k+1} & \cos\lambda l_{k+1} & \sinh\lambda l_{k+1} & \cosh\lambda l_{k+1} \\ -\sin\lambda l_{k+1} & -\cos\lambda l_{k+1} & \sinh\lambda l_{k+1} & \cosh\lambda l_{k+1} \end{bmatrix}. \tag{15a}$$

Substitution of equation (11) into equation (15) and using equation (13) leads to

$$\begin{Bmatrix} 0 \\ 0 \end{Bmatrix} = \underline{B}_{2\times4} \begin{Bmatrix} A_{k+1} \\ B_{k+1} \\ C_{k+1} \\ D_{k+1} \end{Bmatrix} = \underline{B}_{2\times4}\ \underline{T}_{4\times4}^{(k)}\ \underline{T}_{4\times4}^{(k-1)} \cdots \underline{T}_{4\times4}^{(1)} \begin{Bmatrix} A_1 \\ B_1 \\ C_1 \\ D_1 \end{Bmatrix}$$

$$= \underline{R}_{2\times4} \begin{Bmatrix} A_1 \\ B_1 \\ C_1 \\ D_1 \end{Bmatrix} = \begin{bmatrix} r_{11} & r_{12} & r_{13} & r_{14} \\ r_{21} & r_{22} & r_{23} & r_{24} \end{bmatrix} \begin{Bmatrix} A_1 \\ 0 \\ C_1 \\ 0 \end{Bmatrix}, \tag{16}$$

where

$$\underline{R}_{2\times4} = \underline{B}_{2\times4}\ \underline{T}_{4\times4}^{(k)}\ \underline{T}_{4\times4}^{(k-1)} \cdots \underline{T}_{4\times4}^{(1)} = \begin{bmatrix} r_{11} & r_{12} & r_{13} & r_{14} \\ r_{21} & r_{22} & r_{23} & r_{24} \end{bmatrix}.$$

Thus, the existence of non-trivial solutions requires:

$$\det \begin{bmatrix} r_{11}(\lambda) & r_{13}(\lambda) \\ r_{21}(\lambda) & r_{23}(\lambda) \end{bmatrix} = 0. \tag{17}$$

This determinant provides the single (characteristic) equation for the solution of the eigenvalue λ_n. This equation is solved using the standard Newton–Raphson iterations or, for simplification, as shown in Figure 3 to obtain the eigenvalues. The coefficients of the eigenfunctions, $w_n(x)$, are obtained by back substitution into equations (16), (10) and then equation (9).

For the cases of other usually used boundary conditions, through the similar procedure, the following relations can be obtained:

(1) *Cantilever beam*: The existence of non-trivial solutions for the constants A_1, B_1, C_1 and D_1 requires

$$\det \begin{bmatrix} r_{11} - r_{13} & r_{12} - r_{14} \\ r_{21} - r_{23} & r_{22} - r_{24} \end{bmatrix} = 0. \tag{18}$$

The matrix $\underline{B}_{2\times4}$ in equation (15) now becomes

$$\underline{B}_{2\times4} = \begin{bmatrix} -\cos\lambda l_{k+1} & \sin\lambda l_{k+1} & \cosh\lambda l_{k+1} & \sinh\lambda l_{k+1} \\ -\sin\lambda l_{k+1} & -\cos\lambda l_{k+1} & \sinh\lambda l_{k+1} & \cosh\lambda l_{k+1} \end{bmatrix}. \tag{19}$$

(2) *Fixed–fixed beam*: The existence of non-trivial solutions is the same as equation (18) but the matrix $\underline{B}_{2\times4}$ in equation (15) now becomes

$$\underline{B}_{2\times4} = \begin{bmatrix} \sin\lambda l_{k+1} & \cos\lambda l_{k+1} & \sinh\lambda l_{k+1} & \cosh\lambda l_{k+1} \\ \cos\lambda l_{k+1} & -\sin\lambda l_{k+1} & \cosh\lambda l_{k+1} & \sinh\lambda l_{k+1} \end{bmatrix}. \tag{20}$$

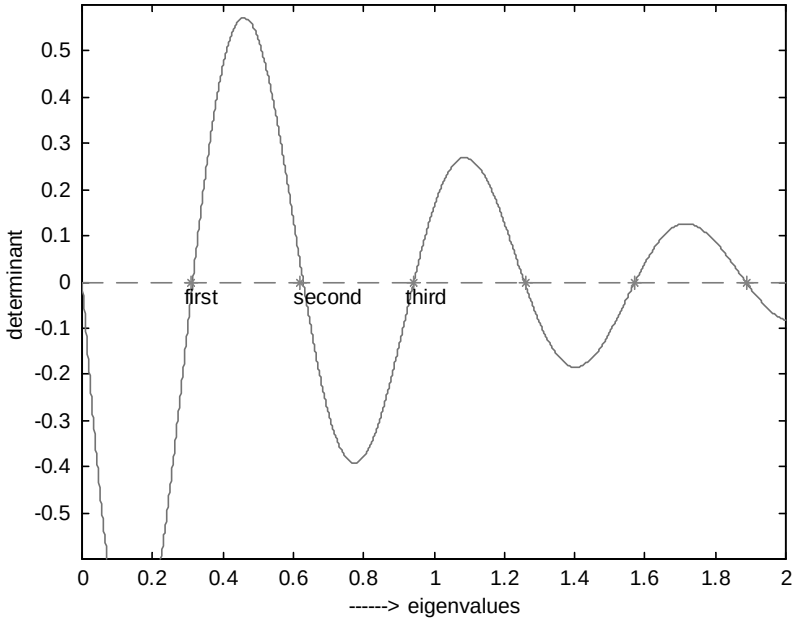

Figure 3. Simple calculation of eigenvalues.

(3) *Free–free beam*: The existence of non-trivial solutions now requires

$$\det \begin{bmatrix} r_{11} + r_{13} & r_{12} + r_{14} \\ r_{21} + r_{23} & r_{22} + r_{24} \end{bmatrix} = 0 \tag{21}$$

and the matrix $\underline{B}_{2\times 4}$ in equation (15) now is the same as equation (19).

4. NUMERICAL RESULTS AND DISCUSSION

The proposed methods are used to solve the beam vibration problems with multiple open cracks (single-sided or double-sided). In order to validate the method in this article, numerical results are compared with the available data. First is the case of the cantilever beam with only one single-sided open crack as in reference [8], the beam L (length) $= 300$ mm, b (width) $= 20$ mm, h (height) $= 20$ mm, Young's modulus $E = 2{\cdot}06 \times 10^{11}$ N/m^2, the density $\rho = 7800$ kg/m^3, the crack is located 140 mm from the fixed end and the crack depth is $a_1 = 10$ mm. From reference [8], the lowest three natural frequencies of this system are measured experimentally as 171, 987 and 3034 Hz [8]. The numerical calculation results by the proposed solution procedure in this article are shown in Table 1. From Table 1, it is observed that the numerical results proposed in this article are satisfactory compared to the experimental data.

By using the proposed method in this article, the eigensolutions of the beam with multiple cracks can be obtained easily. Figures 4–6 present the cases of a cantilever beam with equally spaced cracks (each crack is assumed to have the same depth). Figure 4 shows the curves of the ratio of the first eigenvalue (natural frequency) to uncracked case by increasing the number of cracks N for different crack depths. The same curves of the

TABLE 1

Comparisons for a cantilever beam with one open single-sided crack [8]

Frequency (Hz)	First eigenvalue Ω_1	Second eigenvalue Ω_2	Third eigenvalue Ω_3
Calculated from this article	173·88 Hz	988·45 Hz	3211 Hz
Experimental results from reference [8]	171 Hz	987 Hz	3034 Hz
Error	1·6%	0·15%	5·8%

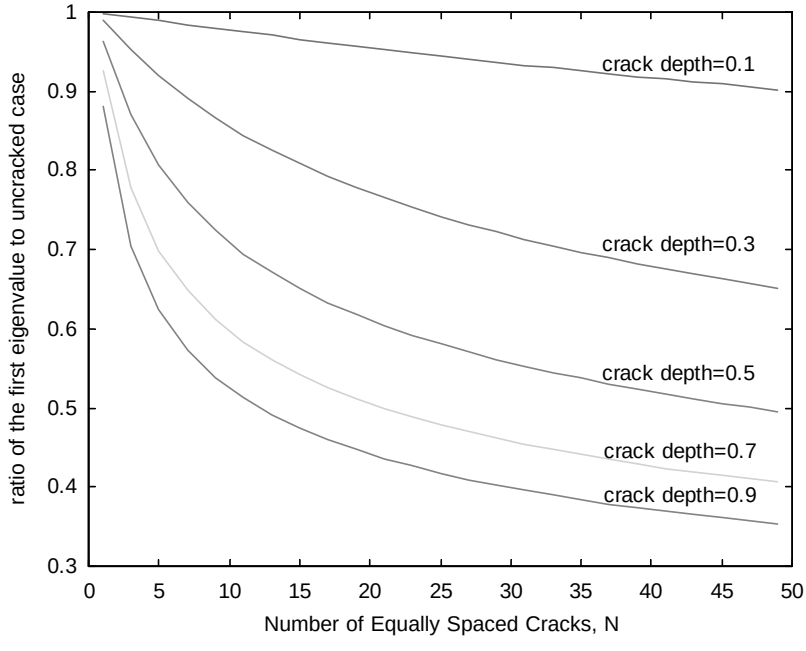

Figure 4. The ratio of the first eigenvalue to the uncracked case for a cantilever beam with equally spaced cracks (each has the same crack depth) as the number of cracks N varies.

second and third eigenvalues are shown in Figures 5 and 6. From these figures, it is observed that three sets of curves in Figures 4–6 are almost coincided when the number of cracks N is large. Note that there are obvious differences for those curves of the small crack number ($N < 5$). That means the variations on eigenvalues are more sensitive when only a few cracks exist. As the number of the cracks N increases, the dynamic behavior becomes more and more insensitive. For another case of a cantilever beam with 49 equally spaced single-sided open cracks which have the same depths, the variations of the lowest three eigenvalues are shown in Figure 7 as the crack depths are changed.

When the eigenvalues are obtained, the corresponding eigenvectors (mode shapes) can also be calculated from equation (9). Figure 8 shows a cantilever beam with five single-sided open cracks. The crack locations and depths are: $x_1 = 0{\cdot}1$, $a_1 = 0{\cdot}5$, $x_2 = 0{\cdot}15$, $a_2 = 0{\cdot}3$, $x_3 = 0{\cdot}2$, $a_3 = 0{\cdot}3$, $x_4 = 0{\cdot}5$, $a_4 = 0.5$ and $x_5 = 0{\cdot}6$, $a_5 = 0{\cdot}3$. By using the method proposed in this article, the lowest three eigenvalues and eigenvectors are shown in Figure 9.

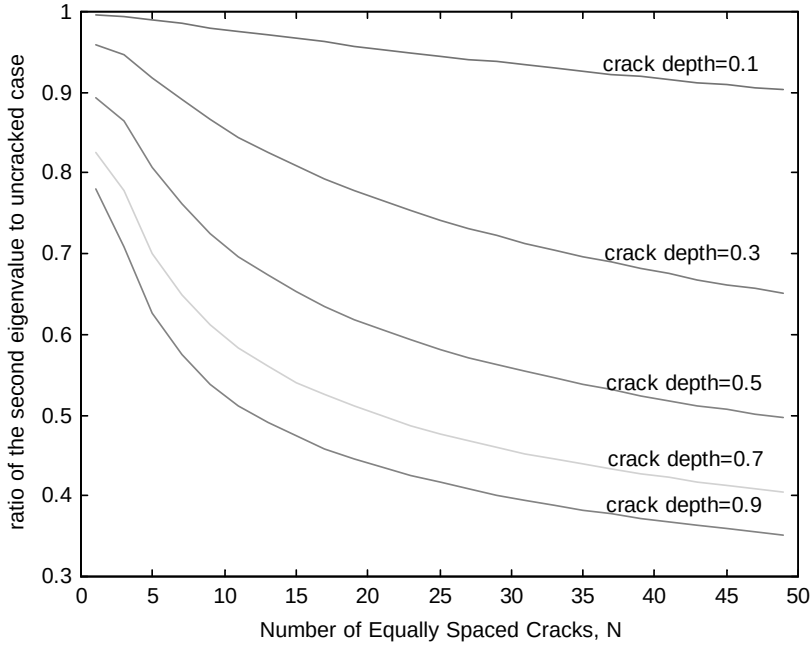

Figure 5. The ratio of the second eigenvalue to the uncracked case for a cantilever beam with equally spaced cracks (each has the same crack depth) as the number of cracks N varies.

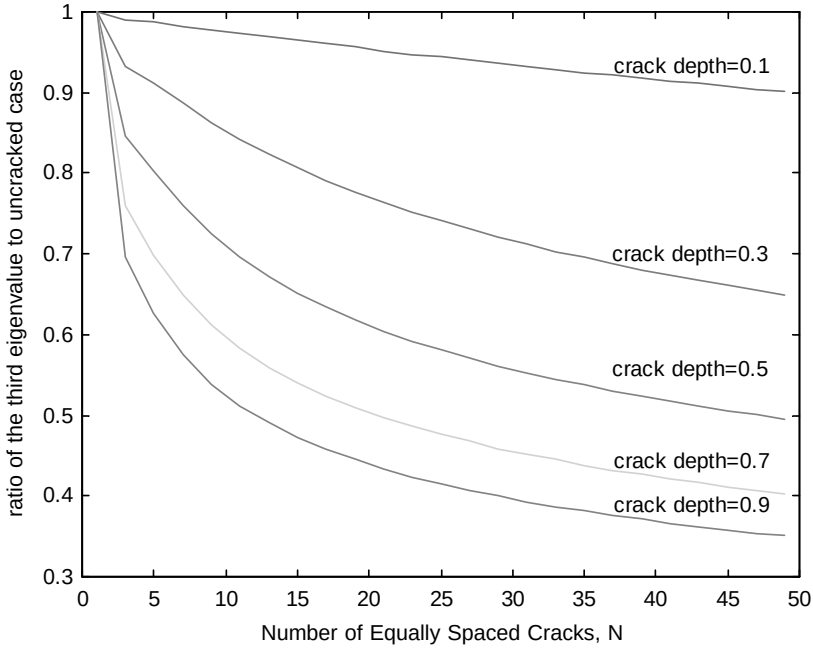

Figure 6. The ratio of the third eigenvalue to the uncracked case for a cantilever beam with equally spaced cracks (each has the same crack depth) as the number of cracks N varies.

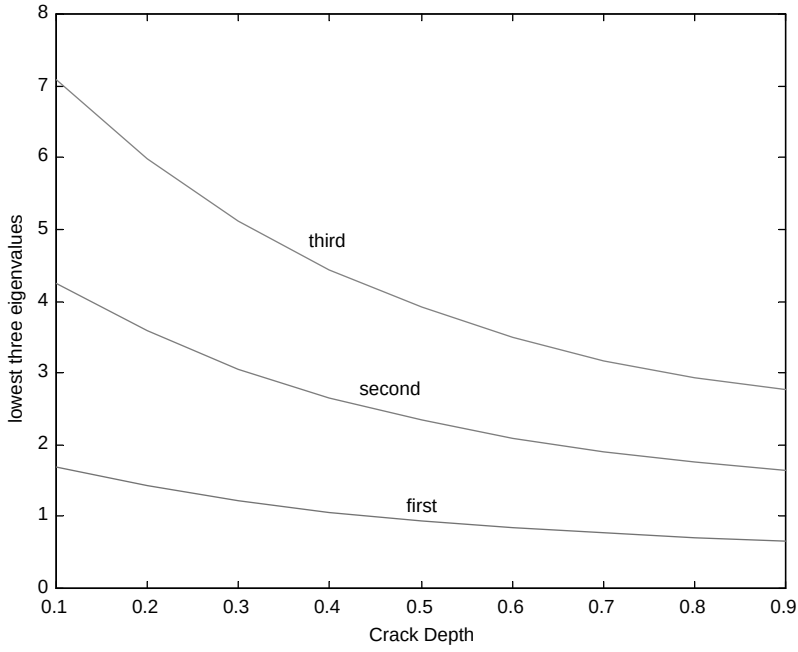

Figure 7. The lowest three eigenvalues of a cantilever beam with 49 single-sided open cracks (each has the same crack depth) by increasing the crack depth.

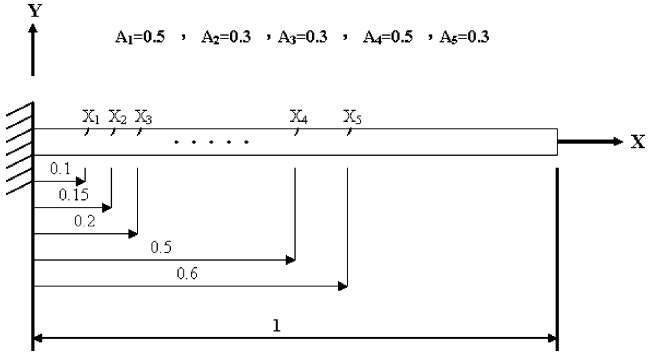

Figure 8. A Cantilever Beam with five cracks: $x_1 = 0{\cdot}1$, $a_1 = 0{\cdot}5$, $x_2 = 0{\cdot}15$, $a_2 = 0{\cdot}3$, $x_3 = 0{\cdot}2$, $a_3 = 0{\cdot}3$, $x_4 = 0{\cdot}5$, $a_4 = 0{\cdot}5$ and $x_5 = 0{\cdot}6$, $a_5 = 0{\cdot}3$.

5. CONCLUSIONS

A hybrid analytical/numerical solution method is developed that permits the efficient evaluation of eigensolutions for a vibration beam with an arbitrary finite number of transverse open cracks. The method utilizes a numerical implementation of a transfer matrix solution to an analytical form of the equation of motion. Unlike all the other methods, in which the dimension of the matrix will increase with the number of cracks, there are only four undetermined coefficients in the method proposed in this article. The dimension of the matrix is independent of the number of cracks in this method. The main

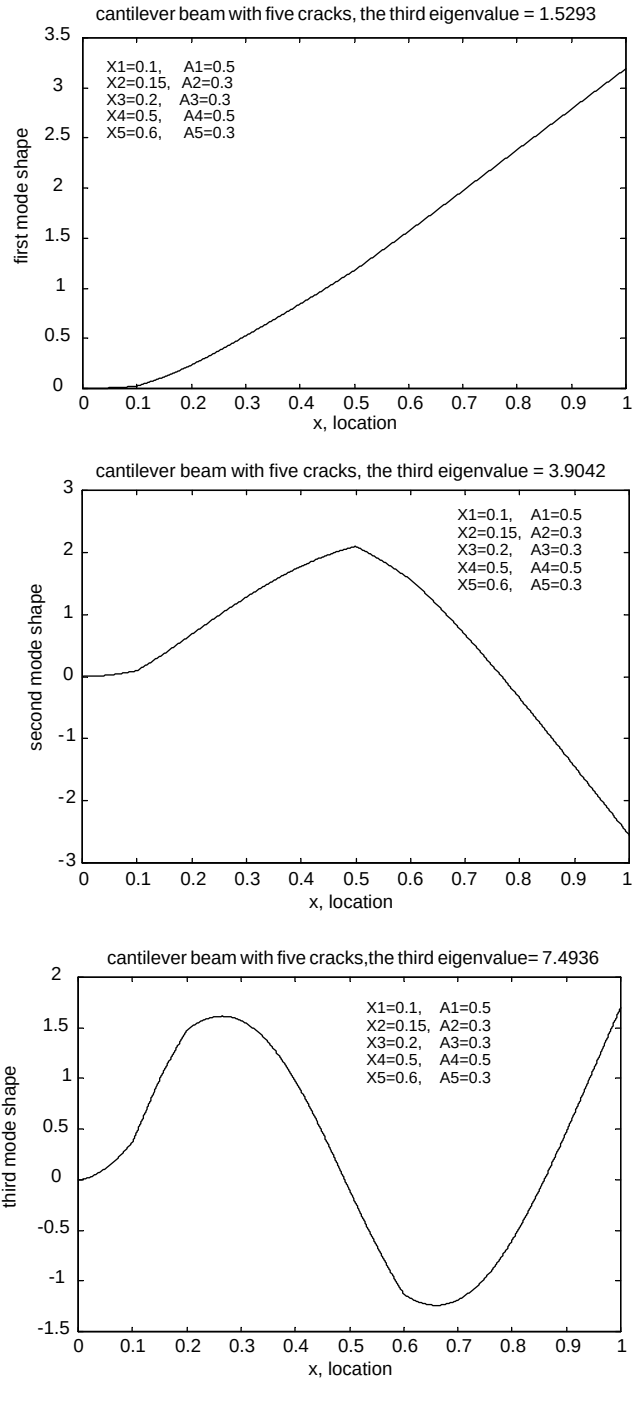

Figure 9. The lowest three mode shapes of a cantilever beam with five single-side open cracks: crack locations and crack depths are: $x_1 = 0{\cdot}1$, $a_1 = 0{\cdot}5$, $x_2 = 0{\cdot}15$, $a_2 = 0{\cdot}3$, $x_3 = 0{\cdot}2$, $a_3 = 0{\cdot}3$, $x_4 = 0{\cdot}5$, $a_4 = 0{\cdot}5$ and $x_5 = 0{\cdot}6$, $a_5 = 0{\cdot}3$.

feature of this method is to decrease the dimension of the matrix involved in the finite element method and some other analytical methods.

ACKNOWLEDGMENTS

The authors gratefully acknowledge the support of the National Science Council of Taiwan R.O.C. under grant number NSC 89-2745-P-212-003.

REFERENCES

1. N. Anifantis and A. D. Dimarogonas 1984 *Computers and Structures* **18**, 351–356. Post buckling behavior of transverse cracked columns.
2. E. I. Shifrin and R. Ruotolo 1999 *Journal of Sound and Vibration* **222**, 409–423. Natural frequencies of a beam with an arbitrary number of cracks.
3. Y. Narkis 1994 *Journal of Sound and Vibration* **172**, 549–558. Identification of crack location in vibrating simply supported beams.
4. B. S. Haisty and W. T. Springer 1988 *Journal of Vibration, Acoustics, Stress, and Reliability in Design* **110**, 389–394. A general beam element for use in damage assessment of complex structures.
5. T. G. Chondros and A. D. Dimarogonas 1980 *Journal of Sound and Vibration* **69**, 531–538. Identification of cracks in welded joints of complex structures.
6. M. H. Shen and C. Pierre 1990 *Journal of Sound and Vibration* **138**, 115–134. Natural modes of Bernoulli–Euler beams with symmetric cracks.
7. W. M. Ostachowitz and M. Krawczuk 1991 *Journal of Sound and Vibration* **150**, 191–201. Analysis of the effect of cracks on the natural frequencies of a cantilever beam.
8. P. F. Rizos and N. Aspragathos 1990 *Journal of Sound and Vibration* **138**, 381–388. Identification of crack location and magnitude in a in cantilever beam from the vibrating modes.
9. M. Boltezar, B. Strancar and A. Kuhelj 1998 *Journal of Sound and Vibration* **211**, 729–734. Identification of transverse crack location in flexural vibrations of free–free beams.
10. A. D. Dimarogonas 1996 *Engineering Fracture Mechanics* **55**, 831–857. Vibration of cracked structures: a state of the art review.
11. T. G. Chondros, A. D. Dimarogonas and J. Yao 1998 *Journal of Sound and Vibration* **215**, 17–34. A continuous cracked beam vibration theory.
12. H. P. Lin and N. C. Perkins 1995 *Journal of Sound and Vibration* **179**, 131–149. Free vibration of complex cable/mass system: theory and experiment.
13. W. C. Hurty and M. F. Rubinstein 1964 *Dynamics of Structures*. Englewood Cliffs, NJ: Prentice-Hall, Inc.
14. H.P. Lin and C. K. Chen 2001 *The 25th National Conference on Theoretical and Applied Mechanics*, 3123–3132. Analysis of cracked beams by transfer matrix method, Taichung, Taiwan.

APPENDIX A: TRANSFER MATRIX DERIVATION

The patching conditions across the ith crack ($i = 1, 2, \ldots, k$) are represented in equations (8a)–(8d). From equations (8a) and (8b), the following can be obtained as

$$B_{i+1} + D_{i+1} = A_i \sin \lambda l_i + B_i \cos \lambda l_i + C_i \sinh \lambda l_i + D_i \cosh \lambda l_i, \quad i = 1, 2, \ldots, k, \tag{A1}$$

$$-B_{i+1} + D_{i+1} = -A_i \sin \lambda l_i - B_i \cos \lambda l_i + C_i \sinh \lambda l_i + D_i \cosh \lambda l_i, \quad i = 1, 2, \ldots, k. \tag{A2}$$

Similarly, equations (8c) and (8d) lead to

$$-A_{i+1} + C_{i+1} = -A_i \cos \lambda l_i - B_i \sin \lambda l_i + C_i \cosh \lambda l_i + D_i \sinh \lambda l_i, \quad i = 1, 2, \ldots, k, \tag{A3}$$

$$A_{i+1} + \theta_i \lambda B_{i+1} + C_{i+1} - \theta_i \lambda D_{i+1} = A_i \cos \lambda l_i - B_i \sin \lambda l_i + C_i \cosh \lambda l_i + D_i \sinh \lambda l_i, \quad i = 1, 2, \ldots, k. \tag{A4}$$

Solving for equations (A1)–(A4) leads to the following recursion formulae for the constants A_{i+1}, B_{i+1}, C_{i+1} and D_{i+1}:

$$\begin{Bmatrix} A_{i+1} \\ B_{i+1} \\ C_{i+1} \\ D_{i+1} \end{Bmatrix} = \begin{bmatrix} t_{11} t_{12} t_{13} t_{14} \\ \vdots \\ \cdots t_{44} \end{bmatrix}^{(i)} \begin{Bmatrix} A_i \\ B_i \\ C_i \\ D_i \end{Bmatrix} = \underline{T}_{4\times4}^{(k-1)} \begin{Bmatrix} A_i \\ B_i \\ C_i \\ D_i \end{Bmatrix}, \quad i = 1, 2, \ldots, k.$$

Here, $\underline{T}_{4\times4}^{(i)}{}_{4\times4}$ is a transfer matrix composed of the elements

$$t_{11} = \cos \lambda l_i - (\tfrac{1}{2})\theta_i \lambda \sin \lambda l_i, \quad t_{12} = -\sin \lambda l_i - (\tfrac{1}{2})\theta_i \lambda \cos \lambda l_i,$$

$$t_{13} = (\tfrac{1}{2})\theta_i \lambda \sin \lambda l_i, \quad t_{14} = (\tfrac{1}{2})\theta_i \lambda \cosh \lambda l_i,$$

$$t_{21} = \sin \lambda l_i, \quad t_{22} = \cos \lambda l_i, \quad t_{23} = 0, \quad t_{24} = 0,$$

$$t_{31} = -(\tfrac{1}{2})\theta_i \lambda \sin \lambda l_i, \quad t_{32} = -(\tfrac{1}{2})\theta_i \lambda \cos \lambda l_i,$$

$$t_{33} = \cosh \lambda l_i + (\tfrac{1}{2})\theta_i \lambda \sinh \lambda l_i, \quad t_{34} = \sinh \lambda l_i + (\tfrac{1}{2})\theta_i \lambda \cosh \lambda l_i,$$

$$t_{41} = 0, \quad t_{42} = 0, \quad t_{43} = \sinh \lambda l_i, \quad t_{44} = \cosh \lambda l_i.$$